Journal of Solid Mechanics Vol. 12, No. 1 (2020) pp. 136-147
DOI: 10.22034/jsm.2019.1866624.1424

Natural Frequency of Rotating Single-Walled Carbon Nanotubes with Considering Gyroscopic Effect

A. Fatahi-Vajari [1,*], Z. Azimzadeh [2]

[1]*Department of Mechanical Engineering, Shahryar Branch, Islamic Azad University, Shahryar, Iran*
[2]*Young Researchers and Elite Club, Yadegar-e-Imam Khomeini (RAH) Shahr-e-Rey Branch, Islamic Azad University, Tehran, Iran*

Received 8 November 2019; accepted 7 January 2020

ABSTRACT

This paper investigates the bending vibration of rotating single-walled carbon nanotubes (SWCNTs) based on nonlocal theory. To this end, the rotating SWCNTs system modeled as a beam with a circular cross section and the Euler-Bernoulli beam theory (EBT) is applied with added effects such as rotary inertia, gyroscopic effect and rotor mass unbalance. Using nonlocal theory, two coupled sixth order partial differential equations that govern the vibration of rotating SWCNTs are derived. To obtain the natural frequency and dynamic response of the nanorotor system, the equation of motion for the rotating SWCNTs are solved. It is found that there are two frequencies in the frequency spectrum. The positive root introduced as forward whirling mode, while the negative root represents backward whirling mode. The detailed mathematical derivations are presented while the emphasis is placed on investigating the effect of the several parameters such as, tube radius, angular velocity and small-scale parameter on the vibration behavior of rotating nanotubes. It is explicitly shown that the vibration of a spinning nanotube is significantly influenced by these effects. To validate the accuracy and efficiency of this work, the results obtained herein are compared with the existing theoretical and experimental results and good agreement is observed. To the knowledge of authors, the vibration of rotating SWCNTs considering gyroscopic effect has not investigated analytically yet and then the results generated herein can be served as a benchmark for future works.

Keywords: Nonlocal theory; Gyroscopic effect; Forward and backward natural frequencies; Scale parameter; Rotating single-walled carbon nanotubes.

1 INTRODUCTION

CARBON nanotubes (CNTs) invented by Iijima [1] are mainly classified into two types namely, single walled carbon nanotubes (SWCNTs) and multi walled carbon nanotubes (MWCNTs). SWCNTs are tiny cylinders

*Corresponding author. Tel.: +98 21 65253183.
E-mail address: afatahiva@yahoo.com (A. Fatahi-Vajari).

made from carbon [2] described as a single layer of a graphite crystal rolled up into a seamless circular cylinder, one atom thickness, usually with a small number of carbon atoms along the circumference and a long length along the cylinder axis [3]. SWCNTs have many unique, fascinating properties. They are very strong and have extremely lightweight. They are excellent conductors of heat, and transport electrons easily. Because of these special properties, they might be used as the substantial parts of nanoelectronics, nanodevices, and nanocomposites. Very often, these components are subjected to external loadings during work operation and their vibrational characteristics and resonant properties are of much concern. Thus, establishing an accurate model considering vibrational properties of nanobeams is an important factor for successful nanostructure design. As a result, nanotechnological research on free vibration properties of nanobeams is important. There have been many studies on the vibration behavior of beam like nanostructures using continuum model [4, 5]. It is proven that the properties of CNTs depend strongly on their microscopic structure [6]. Classical continuum mechanics (CCM) modeling assumptions are deduced to erroneous results, in material domains where the typical microstructural dimension is comparable with the structural ones [7]. Currently, various elegant modifications to CCM have been proposed to consider microstructural features into the theory. These theories are introduced as generalized continuum mechanics [8]. One particular generalized continuum mechanics theory proposed by Eringen is nonlocal theory which states that the stress tensor at a point is a function of strains at all points in the continuum [9]. It is different from the CCM theory which state that the stress at a point is a function of strain at that particular point [10]. Then, in recent years, considerable effort has been devoted to the problem of the vibration of these nanomaterials considering microstructural effects [11]. One of the most modes of vibration for rotating SWCNTs is lateral vibration [12]. Because of wide applications of CNTs, they have potential to be used as new rotating devices such as miniature motor. Ghorbanpour Arani investigated surface and small-scale effects on free transverse vibration of a SWCNT conveying viscose fluid based on nonlocal EBT. The governing equation of motion is solved with the Galerkin method [13]. In another work, Ghorbanpour Arani et al. analyzed vibration and instability of a Y-shaped SWCNT conveying fluid using fourth order beam nonlocal theory [14]. Fatahi-Vajari and Imam studied axial and radial vibration of SWCNT using Doublet mechanics theory [8, 11]. Ghorbanpour Arani et al. presented a realistic model for dynamic instability of embedded SWCNTs conveying pulsating fluid is considering the viscoelastic property of the nanotubes using Kelvin–Voigt model. SWCNTs are placed in longitudinal magnetic fields and modeled by sinusoidal shear deformation beam theory (SSDBT) as well as modified couple stress theory [15]. Ansari et al. studied vibration of SWCNTs using different gradient elasticity theories [16]. The nanostructures that undergo rotation are a system with a promise future to be used in nanomachines which include shaft of nanomotor devices such as fullerene gears and CNT gears [17, 18]. Huang and Han proposed a controllable nanoscale rotating actuator system and investigated its rotating dynamics performance and driving mechanism are through molecular dynamics simulations [19]. Mirtalaie and Hajabasi analyzed the nonlinear axial-lateral-torsional free vibration of the rotating shaft is analyzed by employing the Rayleigh beam theory [20]. Cai et al. investigated Rotation of the inner tube in a double-walled carbon nanotube (DWCNT) system with a fixed outer tube and found to be inducible by a relatively high uniform temperature [21]. Ebrahimi and Shaghaghi employed nonlocal EBT for transverse vibration analysis of an initially pre-stressed size-dependent rotating nanotube [22]. CNTs may be used as rotating machinery in many applications. In general, rotating machinery consists of shafts whose diameters may change with longitudinal position, and bearings placed at various positions in the rotors. In vibration analyses, such a complex nanorotor system should be simplified and a suitable mathematical model is adopted. In the modeling process, it must be known which parameters are important for the system. Nanostructures undergoing rotation include nanoturbines, nanoscale molecular bearings, shaft and gear, and multiple gear systems. These nanostructure machines are expected to receive considerable attention in the near future. Researchers have thus reported the feasibility of nanoscale rotating structures. Examples include study of molecular gears, fullerene gears, and carbon nanotubes gears. Due to the above-mentioned extensive applications and efficacy, the precise prediction of the dynamic behavior of such systems is essential in their safety operation. With the development of high-performance rotating machinery, the need for presenting more and more exact nanorotor dynamic models is increasing. Nowadays, a great effort is devoted to the vibration analysis of nanobeams and CNTS under rotation using the Eringen nonlocal elasticity theory [23-25]. Pradhan and Murmu [26] applied a nonlocal beam model and Differential Quadrature Method (DQM) to investigate the flapwise bending-vibration characteristics of a uniform rotating nanocantilever. Murmu and Adhikari [27] investigated the same problem, but now considering an initially prestressed SWCNT to analyze the effect on the initial preload in the vibration characteristics. Narendar and Gopalakrishnan [28] analyzed the wave dispersion behavior of a uniform rotating nanotube modeled as a nonlocal Euler–Bernoulli beam.

However, much effort is devoted to investigate a rotating nanoscale device, but a preferable model for a nanorotator incorporate gyroscopic effect and scale parameter has not been proposed so far. In the present study, a rotating nanoactuator system is designed based on an analytical model for CNTs using the nonlocal theory. Its

rotational dynamics and physical mechanisms are systematically studied. Furthermore, there is not any attempt to investigate the vibration of CNTs rotates about its own axis. Most of the previous studies on nanorotor dynamics have concentrated on the vibrations behavior of the beams rotating on the fixed hub, solely. As known by authors, the vibrations of rotating SWCNTs rotates on its own axis is not investigated yet, while in these cases a general continuous model in which the effects of lateral deformations with the combination of gyroscopic effects are included is required for providing meaningful results.

As described earlier, both of the above-mentioned factors, namely the geometric property and gyroscopic effect have crucial effects in rotor dynamic analyses. The combination of these effects is the motivation of our work, because many rotor dynamic phenomena include contact or rub impact, crack, gear coupling, misalignment and unbalancement can be investigated based on this model. In this paper, the free vibration of a rotating nanotube is investigated using nonlocal theory. This model contains various factors that could represent the real dynamic behaviors of the system. To this end, the rotating SWCNT is assumed to be attached to supports and is undergoing rotation about its axis. Nonlocal EBT is employed to formulate the governing equations. The basic equation of motion for vibration of rotating SWCNTs which considers small-scale effect is obtained. After that, this equation is solved to give the natural frequencies of rotating SWCNTs.

2 EQUATIONS OF MOTION FOR ROTATING NANOTUBES USING NONLOCAL THEORY

A rotating CNT can be represented as a cantilever beam having displacements perpendicular to the plane of rotation. The model is established based on the EBT in which the effects of rotary inertia and gyroscopic forces are added but the shear deformation is neglected. The latter assumption means that the deformation due to the shear force can be neglected and the former assumption makes it possible to calculate the strain at an arbitrary position in the beam. In this theory, the bending moment at an arbitrary position of the beam is proportional to the inverse of the radius of curvature of the centerline of the beam and only the lateral motion is considered. For slender rotors, EBT expresses the motion of the rotor, suitably. It is known that when the wave length of the vibration mode becomes small relative to the beam thickness, the effect of rotary inertia and that of the deformation due to shearing forces, called shear deformation, appear. A beam model taking these two effects into account is called the Timoshenko beam. In a rotor system, when the diameter-to-length ratio increases, these two effects appear in addition to the effect of the gyroscopic moment.

CNT can be considered as an elastic rotor whose diameter doesn't vary much and modeled appropriately by distributed parameter model. In the following, this model, which has distributed mass, distributed stiffness and distributed damping, called a continuous carbon nanotube rotor (CCNTR). Analysis of CCNTRs is based on the theory of beam's lateral vibrations. In recent years, one main concern for researchers is to predict the critical speed, because the first thing that had to be done in designing rotating machinery is to avoid resonance. In rotor dynamics, the rotating speeds that produce resonance responses are called critical speeds. The deformation of a nanorotor is the highest in the neighborhood of the critical speed. It should be pointed out that rotor is often used as the general term for the rotating part of a rotating machine. The opposite term is stator, which means the static part of the machine. If a flexible nanorotor with distributed mass and stiffness is considered, this model is called a distributed-parameter system or continuous nanorotor system. Rotors are sometimes classified into vertical and horizontal shaft systems. In this paper, it is discussed the vertical model but the effect of gravity is ignored. Fig. 3 shows the theoretical model of an elastic CCNTR with a circular cross section. The length of this uniform rotor is l. As the rotor is supported vertically, gravitational force does not work however in horizontal case, gravitational force may be ignored. For simplicity, shear deformation is not considered.

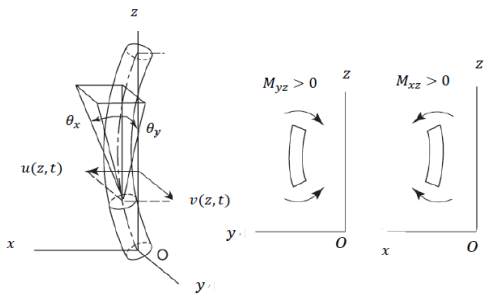

Fig.1
A rotor.

The rectangular coordinate system $O-xyz$ is fixed in space. The axis along the nanorotor centerline is represented by *z* because *s* is used as a complex variable representing the deflection of the rotor in the following. The deflections in the *x* and *y* directions at the position *z* are denoted by and, respectively. The displacement fields in any section of the nanobeam are expressed by [23]

$$u_x = u(z,t), u_y = v(z,t), u_z = x\frac{\partial u(z,t)}{\partial z} + y\frac{\partial v(z,t)}{\partial z} \tag{1}$$

The inclination angle $\theta(z,t)$ of the tangent to the nanorotor deflection curve is represented by two components $\theta_x(z,t)$ and $\theta_y(z,t)$, which are the projections of θ to the xoz and yoz planes, respectively, and are given by [17]

$$\theta_x = \frac{\partial u}{\partial z}, \theta_y = \frac{\partial v}{\partial z} \tag{2}$$

Let the moments working in the xoz and yoz planes be M_{xz} and M_{yz}, respectively. From the EBT, the following relationships between M_{xz}, M_{yz} and θ_x, θ_y in the scale less condition, are expressed [23]

$$M_{xz} = EI\frac{\partial \theta_x}{\partial z}, M_{yz} = EI\frac{\partial \theta_y}{\partial z} \tag{3}$$

where *E* is Young's modulus and *I* is the cross-sectional area moment of inertia.

The signs of the bending moments M_{xz} and M_{yz} are defined as positive when they work to increase θ_x and θ_y as *z* increases, as shown in Fig. 1. The relation between stress with force and moments are expressed by the following equations [23]:

$$F_x = \int_0^L \sigma_{xz}\, dA, F_y = \int_0^L \sigma_{yz}\, dA \tag{4}$$

$$M_{xz} = \int_0^L x\,\sigma_{zz}\, dA, M_{yz} = \int_0^L y\,\sigma_{zz}\, dA \tag{5}$$

Now, the scale effect is entered to the problem under study using Eringen nonlocal theory. According to Eringen theory [1–3], the stress field at a point x in an elastic continuum not only depends on the strain field at the point but also on strains at all other neighboring points of the body. Eringen attributed this fact to the atomic theory of lattice dynamics and experimental observations on phonon dispersion. The nonlocal stress tensor σ at point *x* is expressed as [9]

$$\sigma = \int_V K(|\boldsymbol{x}-\boldsymbol{x}'|,\tau)\boldsymbol{t}(\boldsymbol{x}')d\boldsymbol{x}' \tag{6}$$

where $\boldsymbol{t}(\boldsymbol{x})$ is the classical, macroscopic stress tensor at point *x* and the kernel function $K(\boldsymbol{x}-\boldsymbol{x}',\tau)$ represents the nonlocal modulus, $|\boldsymbol{x}-\boldsymbol{x}'|$ being the distance (in Euclidean norm) and τ is a material constant that depends on internal and external characteristic lengths (such as the lattice spacing and wavelength, respectively). The macroscopic stress *t* at a point *x* in a Hookean solid is related to the strain ε at the point by the generalized Hooke's law [7]

$$\boldsymbol{t}(\boldsymbol{x}) = C(\boldsymbol{x}) : \varepsilon(\boldsymbol{x}) \tag{7}$$

where C is the fourth-order elasticity tensor and : denotes the 'double-dot (tensor) product. The constitutive Eqs. (6) and (7) together define the nonlocal constitutive behavior of a Hookean solid. Eq. (6) represents the weighted average of the contributions of the strain field of all points in the body to the stress field at a point. The integral constitutive relation in Eq. (6) makes the elasticity problems difficult to solve. However, it is possible to represent the integral constitutive relations in an equivalent differential form as [15]

$$\sigma - \eta^2 \nabla^2 \sigma = \boldsymbol{t}, \eta = e_0 a \tag{8}$$

where e_0 and a are a material constant and the internal characteristic lengths, respectively. Using Eqs. (7) and (8), stress resultants can be expressed in terms of the scale parameter. As opposed to the linear algebraic equations between the stress resultants and strains in a local theory, the nonlocal theory results in differential relations involving the stress resultants and the strains. In the following, these relations are presented for homogeneous isotropic nanobeams under the assumption that the nonlocal behavior is negligible in the thickness direction. Then, the nonlocal constitutive relation in Eq. (8), with Eq. (7) for the macroscopic stress, takes the following special relations for nanobeams:

$$\sigma_{xz} - \eta^2 \frac{\partial^2 \sigma_{xz}}{\partial z^2} = E\,\varepsilon_{xz}, \sigma_{yz} - \eta^2 \frac{\partial^2 \sigma_{yz}}{\partial z^2} = E\,\varepsilon_{yz} \tag{9}$$

where E is Young's modulus of the beam. It is clear that when the nonlocal parameter η is zero, the constitutive relations of the local theories are obtained.

Form Eq. (1), the strains of the rotating nanobeam are obtained as follow:

$$\varepsilon_{xz} = \frac{\partial u}{\partial z}, \varepsilon_{yz} = \frac{\partial v}{\partial z}, \varepsilon_{zz} = x \frac{\partial^2 u}{\partial z^2} + y \frac{\partial^2 v}{\partial z^2} \tag{10}$$

Substituting Eq. (9) into Eq. (4) with using Eq. (10) yields the following nonlocal shear forces for the nanorotor

$$F_x - \eta^2 \frac{\partial^2 F_x}{\partial z^2} = EA \frac{\partial u}{\partial z}, F_y - \eta^2 \frac{\partial^2 F_y}{\partial z^2} = EA \frac{\partial v}{\partial z} \tag{11}$$

Similarly, the nonlocal shear moments are obtained with substituting Eq. (9) into Eq. (5) along with using Eq. (10) as:

$$M_{xz} - \eta^2 \frac{\partial^2 M_{xz}}{\partial z^2} = EI \frac{\partial^2 u}{\partial z^2}, M_{yz} - \eta^2 \frac{\partial^2 M_{yz}}{\partial z^2} = EI \frac{\partial^2 v}{\partial z^2} \tag{12}$$

To derive the equations of motion, a sliced element with thickness dz at z is considered as shown in Fig. 2.

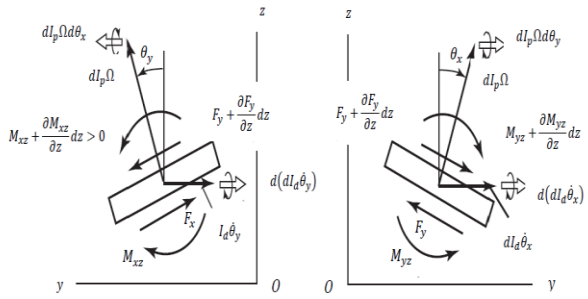

Fig.2
Component of moments.

The polar moment of inertia dI_p and the diametric moment of inertia dI_d of this element are given by [23]:

$$dI_p = (\rho A\, ds)\frac{R^2}{2}, dI_d = \frac{dI_p}{2} = (\rho A\, ds)\frac{R^2}{4} \tag{13}$$

where R is the radius of the rotor, A the cross-sectional area, and ρ the density of the shaft material.

Now, the correspondence equations of motion for the nanorotor are obtained using this sliced element. Suppose that the nanorotor is executing a whirling motion and the inclination of the sliced element changes from θ_x to $\theta_x + d\theta_x$ and from θ_y to $\theta_y + d\theta_y$, respectively, during time dt. Changes in the angular momentums about the principal axes of the moment of inertia are shown in Fig. 2. The shearing force $F(z,t)$ and the moment $M(z,t)$ are also shown in Fig. 2. The equations of motion are obtained from the relationships among momentum and angular momentum changes, and shearing forces and moments, as follows. In the first, the lateral motion of a sliced element is considered. Let the viscous damping coefficient per unit length of the rotor be c, the deflection of the center of gravity at the position z be (u_G, v_G), and the components of a force in the x- and y-directions be F_x and F_y, respectively. Newton's second law gives

$$(\rho A\, dz)\frac{\partial^2 u_G}{\partial t^2} = -F_x + \left(F_x + \frac{\partial F_x}{\partial z}dz\right) - c\frac{\partial u}{\partial t}dz \tag{14}$$

$$(\rho A\, dz)\frac{\partial^2 v_G}{\partial t^2} = -F_y + \left(F_y + \frac{\partial F_y}{\partial z}dz\right) - c\frac{\partial v}{\partial t}dz \tag{15}$$

After making some manipulations, the following equations are obtained

$$\rho A\frac{\partial^2 u_G}{\partial t^2} + c\frac{\partial u}{\partial t} = \frac{\partial F_x}{\partial z} \tag{16}$$

$$\rho A\frac{\partial^2 v_G}{\partial t^2} + c\frac{\partial v}{\partial t} = \frac{\partial F_y}{\partial z} \tag{17}$$

It should be pointed out that unbalance is defined as the condition which exists in a nanorotor when vibratory force or motion is imparted to its bearings as a result of centrifugal force. One main cause of vibrations is the excitation due to inevitable mass unbalance of nanorotors. Residual unbalance usually occurs owing to various causes such as synthesis error, thermal deformation, material inhomogeneity and so on. It also occurs owing to stuck up of tolerance in assembly. When a well-balanced rotor is mounted on a well-balanced shaft, the necessary assembly tolerances permit radial displacement of the nanorotor, and, as a result, unbalance occurs. The term unbalance refers to the nonuniform distribution of the mass of a rotor about its axis of rotation.

Next, the inclination motion is considered. The components in the xoz and yoz planes indicated by the vectors are shown in Fig. 2. The moment vectors in the x- and y-directions are composed of the moments working on the element and the moments due to the shearing forces. From the relationships between the variations in angular momentum during dt and the applied moments in the x- and y-directions, the following expressions are obtained:

$$\frac{d\left(dI_d\dot{\theta}_x\right) + dI_d\Omega d\left(d\theta_y\right)}{dt} = -M_{xz} + \left(M_{xz} + \frac{\partial M_{xz}}{\partial z}dz\right) + F_y dz \tag{18}$$

$$\frac{-d\left(dI_d\dot{\theta}_y\right) + dI_d\Omega d\left(d\theta_x\right)}{dt} = -M_{yz} + \left(M_{yz} + \frac{\partial M_{yz}}{\partial z}dz\right) + F_x dz \tag{19}$$

where $F_x dz$ and $F_y dz$ represent moments due to the shearing forces. Substituting Eq. (2) into Eqs. (18) and (19) and making some manipulations, the following equation are obtained

$$\left(\frac{dI_d}{dz}\right)\frac{\partial^3 u}{\partial z\,\partial t^2}+\left(\frac{dI_p}{dz}\right)\Omega\frac{\partial^2 v}{\partial z\,\partial t}=\frac{\partial M_{xz}}{\partial z}+F_x \tag{20}$$

$$\left(\frac{dI_d}{dz}\right)\frac{\partial^3 v}{\partial z\,\partial t^2}-\left(\frac{dI_p}{dz}\right)\Omega\frac{\partial^2 u}{\partial z\,\partial t}=\frac{\partial M_{yz}}{\partial z}+F_y \tag{21}$$

In the above equations, the first terms are due to the rotary inertia and the second terms appear because of the gyroscopic moment. By differentiating these equations with respect to z and substituting Eqs. (16) and (17) into them to eliminate F_x and F_y , the following equations are obtained:

$$\left(\frac{dI_d}{dz}\right)\frac{\partial^4 u}{\partial z^2\partial t^2}+\left(\frac{dI_p}{dz}\right)\Omega\frac{\partial^3 v}{\partial z^2\partial t}=\frac{\partial^2 M_{xz}}{\partial z^2}+\rho A\frac{\partial^2 u_G}{\partial t^2}+c\frac{\partial u}{\partial t} \tag{22}$$

$$\left(\frac{dI_d}{dz}\right)\frac{\partial^4 v}{\partial z^2\partial t^2}-\left(\frac{dI_p}{dz}\right)\Omega\frac{\partial^3 u}{\partial z^2\partial t}=\frac{\partial^2 M_{yz}}{\partial z^2}+\rho A\frac{\partial^2 v_G}{\partial t^2}+c\frac{\partial v}{\partial t} \tag{23}$$

Using Eqs. (22) and (23) and expressing the components M_{xz} and M_{yz} from Eq. (12) as u and v, the following equations of motion are obtained:

$$I_{d0}\frac{\partial^4 u}{\partial z^2\partial t^2}+I_{p0}\Omega\frac{\partial^3 v}{\partial z^2\partial t}=\eta^2\left(I_{d0}\frac{\partial^6 u}{\partial z^4\partial t^2}+I_{p0}\Omega\frac{\partial^5 v}{\partial z^4\partial t}-\rho A\frac{\partial^4 uc}{\partial z^2\partial t^2}-c\frac{\partial^2 u}{\partial z^2\partial t}\right)+EI_{d0}\frac{\partial^4 u}{\partial z^4}+\rho A\frac{\partial^4 uc}{\partial t^2}+c\frac{\partial u}{\partial t} \tag{24}$$

$$I_{d0}\frac{\partial^4 v}{\partial z^2\partial t^2}-I_{p0}\Omega\frac{\partial^3 u}{\partial z^2\partial t}=\eta^2\left(I_{d0}\frac{\partial^6 v}{\partial z^4\partial t^2}-I_{p0}\Omega\frac{\partial^5 u}{\partial z^4\partial t}-\rho A\frac{\partial^4 vc}{\partial z^2\partial t^2}-c\frac{\partial^2 v}{\partial z^2\partial t}\right)+EI_{d0}\frac{\partial^4 v}{\partial z^4}+\rho A\frac{\partial^4 vc}{\partial t^2}+c\frac{\partial v}{\partial t} \tag{25}$$

where $I_{d0}=\frac{dI_d}{dz}, I_{p0}=\frac{dI_p}{dz}$. For the nanotube under study $I_{d0}=\frac{\pi}{4}\left(R_o^4-R_i^4\right), I_{p0}=\frac{\pi}{2}\left(R_o^4-R_i^4\right)$.

Introducing $s=u+iv$ and $s_G=u_G+iv_G$, the above equations can be simplified to Eq. (26)

$$I_{d0}\frac{\partial^4 s}{\partial z^2\partial t^2}-I_{p0}\Omega\frac{\partial^3 s}{\partial z^2\partial t}i=\eta^2\left(I_{d0}\frac{\partial^6 s}{\partial z^4\partial t^2}-iI_{p0}\Omega\frac{\partial^5 s}{\partial z^4\partial t}-\rho A\frac{\partial^4 sc}{\partial z^2\partial t^2}-c\frac{\partial^2 s}{\partial z^2\partial t}\right)+EI_{d0}\frac{\partial^4 s}{\partial z^4}+\rho A\frac{\partial^4 sc}{\partial t^2}+c\frac{\partial s}{\partial t} \tag{26}$$

This equation is the basic equation for the vibration of rotating SWCNT considering scale effect. The boundary conditions may be categorized as follow:

Simply supported boundary conditions: $s=0, s''=0$

Fixed boundary conditions: $s=0, s'=0$

Free boundary conditions: $s'=0, s''=0$

3 SOLVING THE EQUATION OF MOTION

The boundary conditions of the tube are assumed to be simply supported. Then, to find the frequency of RBLMS of the nanotube, the solutions for the vibrations of rotating SWCNT are assumed to be of the form

$$s = S\sin\left(\frac{n\pi}{L}z\right)e^{i\omega t} \tag{27}$$

where S and $\omega^{(\eta)}$ are the amplitude and angular frequency of the rotating nanobeam vibration, respectively. n is the vibration mode. $\omega^{(\eta)}$ may be related to natural frequency f by $\omega^{(\eta)} = 2\pi f$. Superscript η in $\omega^{(\eta)}$ indicates the natural frequency incorporates scale effects.

Substituting Eq. (27) into Eq. (26) yields

$$I_{d0}\left(\frac{n\pi}{L}\right)^2\omega^2 - I_{p0}\Omega\left(\frac{n\pi}{L}\right)^2\omega = \eta^2\left(-I_{d0}\left(\frac{n\pi}{L}\right)^4\omega^2 + I_{p0}\Omega\left(\frac{n\pi}{L}\right)^4\omega - \rho A\left(\frac{n\pi}{L}\right)^2\omega^2 + ic\omega\left(\frac{n\pi}{L}\right)^2\right) + EI_{d0}\left(\frac{n\pi}{L}\right)^4 - \rho A\omega^2 + ic\omega \tag{28}$$

Then, with solving Eq. (28), two roots ω_{1n} and ω_{2n} are obtained which include the scale parameter η and rotating speed Ω . With neglecting the eccentricity and damping effect, these two equations are as follow:

$$\omega_n^{\eta} = \frac{A\Omega \pm \sqrt{A^2\Omega^2 + 4BC}}{2B} \tag{29}$$

wherein *A, B* and *C* are defined by the following equations

$$A = I_{p0}\left(\frac{n\pi}{L}\right)^2 + I_{p0}\Omega\left(\frac{n\pi}{L}\right)^4 \tag{30}$$

$$B = I_{d0}\left(\frac{n\pi}{L}\right)^2 + \eta^2 I_{d0}\left(\frac{n\pi}{L}\right)^4 + \eta^2\rho A\left(\frac{n\pi}{L}\right)^2 + \rho A \tag{31}$$

$$C = EI_{d0}\left(\frac{n\pi}{L}\right)^2 \tag{32}$$

Eq. (28) is the natural frequency for the rotating vibration of a SWCNT incorporating the gyroscopic and scale effects. In Eq. (29), ω_n is the natural frequency corresponding to the *n*th mode. The advantage of this simple expression is that it explicitly shows the dependency of the natural frequency of rotating SWCNTs on the mechanical and geometrical properties. According to Eq. (29), there are two frequencies in the frequency spectrum. The positive root ω_{1n} represents a frequency of a forward whirling mode, while the negative root ω_{2n} represents that of a backward whirling mode. It can be concluded that for infinite diameters, ω_1 which correspond to a transverse acoustic mode has zero frequency and ω_2 which correspond to the breathing mode of a bi-layer of graphene has the following frequency

$$\omega_2 = \frac{\sqrt{EI_{d0}\left(\frac{n\pi}{L}\right)^4\left[I_{d0}\left(\frac{n\pi}{L}\right)^2 + \eta^2 I_{d0}\left(\frac{n\pi}{L}\right)^4 + \eta^2\rho A\left(\frac{n\pi}{L}\right)^2 + \rho A\right]}}{2\left(I_{d0}\left(\frac{n\pi}{L}\right)^2 + \rho A\right)} \tag{33}$$

which is equal to the frequency obtained in [15]. On the other hand, If the scale effect is neglected means $\eta = 0$, the natural frequencies will be

$$\omega_{1n}^{\eta},\omega_{2n}^{\eta}=\left(\frac{n\pi}{L}\right)^2\frac{I_{p0}\Omega\pm\sqrt{{I_{p0}}^2\Omega^2+4EI_{d0}\left(I_{d0}\left(\frac{n\pi}{L}\right)^2+\rho A\right)}}{2\left(I_{d0}\left(\frac{n\pi}{L}\right)^2+\rho A\right)} \tag{34}$$

which is in complete agreement with the natural frequency obtained in [23].

It should be noted that he intersections of the straight line $\omega=\Omega$ and the curves ω_n give the major critical speeds ω_n. Setting $p_n=\Omega=\omega_n$ in Eq. (29), it is obtained that

$$\Omega=\frac{A+\sqrt{A^2+BC}}{B} \tag{35}$$

Since ω_n is real only when the quantity under the radical sign in the denominator is positive, the major critical speed does not exist for higher modes with large *n*. Eq. (35) indicates that because of scale parameter and rotating speed, there are major differences between the predictions of present work and the other models. These differences will be explained in the next section.

4 RESULTS AND DISCUSSION

In this section, comparison between the results obtained using present work and molecular dynamics (MD) and CCM results are presented. Experimentally, the frequency is related to ω via $f=\frac{w}{2\pi C}$ where, $C=2.99\times10^{10}\frac{cm}{s}$ is the velocity of light in the vacuum [8]. This relation is used in Table 1., below to report the frequencies in cm^{-1}.Throughout this paper, the material properties of SWCNT are taken to be: Young's modulus $E=1TPa$, mass density $\rho=2300\frac{kg}{m^3}$ and Poisson's ratio $\nu=0.2$ [3]. In this paper, the scale parameter used is the carbon-carbon bond length $\eta=0.1421nm$ [6]. Table 1., shows the frequencies of (8, 8) Armchair SWCNTs for 10 different aspect ratios based on the available experimental and analytical results. The first column shows the aspect ratios of the nanotube and the next three columns are the experimental and analytical results from the CCM and nonlocal model (the present work), respectively.

From Table 1., it can be seen that the doublet mechanical predictions of the natural frequencies of different rotating SWCNTs are in good agreement with the available experimental results.

Table 1
Fundamental frequencies (THz) for (8, 8) Armchair SWCNTs obtained from MD simulations and different gradient Euler–Bernoulli beam models for $\Omega=0$.

Aspect ratio	MD [15]	CCM	Present work
8.3	0.5299	0.5380	0.5378
10.1	0.3618	0.3640	0.3639
13.7	0.1931	0.1982	0.1982
17.3	0.1103	0.1244	0.1244
20.9	0.0724	0.0853	0.0853
24.5	0.0519	0.0621	0.0621
28.1	0.0425	0.0472	0.0472
31.6	0.0358	0.0373	0.0373
35.3	0.0287	0.0299	0.0299
39.1	0.0259	0.0244	0.0244

The forward and backward frequencies obtained in the previous section by the present methods are also compared in graphic form in Figs. 3-6. In these figures the nanotubes is considered to be Zigzag (16, 0) SWCNT

with simply supported boundary condition. As shown in these figures, the two frequencies are very sensitive to the diameter d of the SWCNT, when this geometrical property is extremely small. The two frequencies decrease considerably with increasing tube diameter.

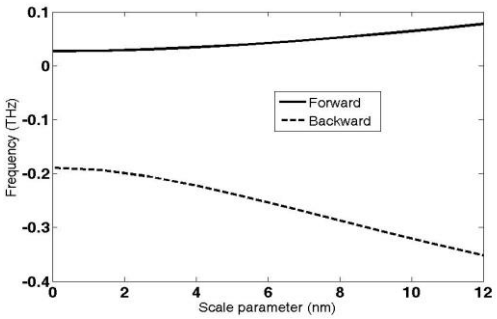

Fig.3
Variation of the forward and backward frequencies with scale parameter.

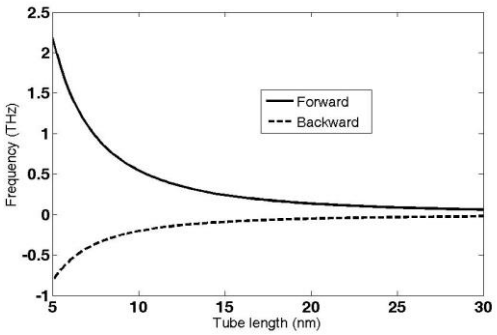

Fig.4
Variation of the forward and backward frequencies with tube length.

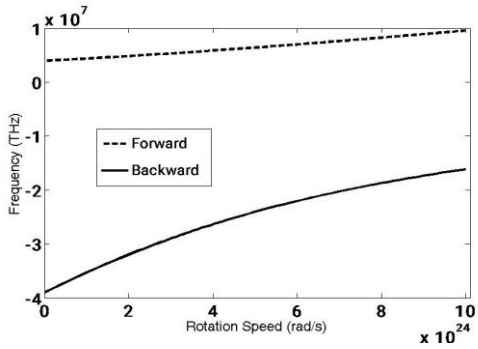

Fig.5
Variation of the forward and backward frequencies with rotating speed.

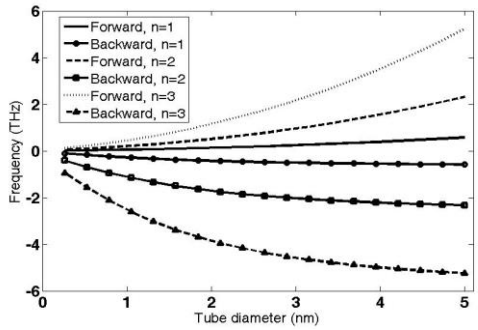

Fig.6
Variation of the forward and backward frequencies with tube diameter.

In Fig. 3, the effect of scale parameter on the two frequencies in different vibration modes is shown for. The boundary conditions of the nanotubes are assumed to be simply support. It is found that the forward frequency increases with increasing in scale parameter. This decreasing is more apparent for higher scale parameter. Inverse effect is seen for backward frequency. In Fig. 4 variation of the two frequencies with tube length is shown.

According to this figure, increase in the length of the nanotube results in increase in the backward frequency. This increase is more apparent for lower tube length. Inverse effect is seen for forward frequency. Since scale effect is more apparent for smaller wave lengths, beyond a certain tube length, both forward and backward frequencies approach to certain values. This figure also shows that at large length, the discrepancy between the forward and backward frequencies becomes small. It can also be seen that the forward frequency is larger than the stationary tube while the backward frequency is smaller.

The frequencies variation against rotation speed of rotating SWCNT is illustrated in Fig. 5. It can also be seen that as the rotation speed increases, both forward and backward frequencies increase. This increasing is more apparent for backward frequency. It can also be seen from that in contrast to stationary systems, the frequency is a function of rotation speed so that the larger the rotation speed, the more pronounced the discrepancy between the stationary and rotating frequencies becomes. Variations of the forward and backward frequencies with tube diameter are drawn in Fig. 6 for different mode numbers. As the tube diameter increases, the backward frequency decreases. This reduction is more significant for higher vibration modes and in lower tube diameters. As the tube diameter increases more, the backward frequencies tend to approach to constant values. On the other hand, the inverse effect was seen for the forward frequencies. The forward frequencies increase as the tube diameter increases. The increasing effect is more apparent for higher mode numbers and diameters. It can also be seen that for the same diameters, with increasing mode numbers, forward frequencies increase while backward frequencies decrease.

5 CONCLUSIONS

In this paper, a detailed investigation of the natural frequency of the rotating SWCNT based on nonlocal theory has been presented. The equation of motion for vibration of the rotating SWCNT based on nonlocal theory is derived. To obtain the frequency equation in rotating SWCNT vibration, the equation of motion for SWCNTs with simply supported end conditions is solved. The significant dependency of this oscillation to tube geometry, rotating speed and the scale parameter are observed. To show the accuracy and capability of this method, the generated results obtained herein have been compared with those available in open literature, and excellent correlation has been achieved. The following points are particularly noted.

1. Due to the coupling of the vibrations in x and y directions and obtaining the forward and backward linear natural frequencies in lateral modes of vibrations, backward and forward nonlinear natural frequencies are defined in the analysis.
2. The inclusion of the nonlocal effect increases the forward natural frequency and decreases backward natural frequency. As shown in this study, the nonlocal effect is considerably different and more pronounced in the higher vibration modes.
3. The natural frequencies of the system are obtained as the functions of scale parameter which this phenomenon is due to microstructural nature of the system. The scale parameter affects the natural frequencies in the decimal digits in comparison with the continuum natural frequencies. Also, this effect is more evident in the upper natural frequencies than their lower modes.
4. For a same rotating speed, the values of the natural frequencies in forward and backward modes are close together but they differ at the higher modes from each other. The difference between the forward and backward natural frequencies is more evident in lower rotating speeds.
5. The results showed that the increase or decrease in the natural frequencies of the rotor is well matched with the rotor speed. It was seen that the natural frequencies increase very slowly by increasing of the shaft spin speed. The rotating speed affects the higher natural frequencies more.
6. The forward natural frequencies decrease by the increase in the value of the shaft length. An inverse effect is seen in the backward frequencies. This effect is more observed in lower tube lengths. As the length increases more, the two frequencies converge to a single value.
7. The backward natural frequencies decrease by the increase in the value of the tube diameter. An inverse effect is seen in the forward frequencies. This effect is more observed in higher mode numbers.
8. The effect of the scale parameter on the natural frequencies is intensified as the higher modes are excited also for higher spin speeds of the rotor. In general, it is seen that the natural frequencies are relatively coincident in the lower mode numbers, but they deviate more in higher modes. This shows that the effect of interaction between frequencies is more evident at higher vibration modes.

9. In lateral modes of vibrations, the variation of the forward natural frequencies with respect to the rotation speed has a linear form in its lower values while the variations become of higher order than the linear form as the values of rotation speed becomes larger, especially in the backward modes.

REFERENCES

[1] Iijima S., 1991, Helical microtubes of graphitic carbon, *Nature* **354**: 56-58.

[2] Basirjafari S., Khadem S. E., Malekfar R., 2013, Radial breathing mode frequencies of carbon nanotubes for determination of their diameters, *Current Applied Physics* **13**: 599-609.

[3] Fatahi-Vajari A., 2018, A new method for evaluating the natural frequency in radial breathing like mode vibration of double-walled carbon nanotubes, *ZAMM* **98**(2): 255-269.

[4] Rao S. S., 2000, *Mechanical Vibrations*, Addison-Wesley Publishing Company, Massachusetts.

[5] Gupta S. S., Bosco F. G., Batra R. C., 2010, Wall thickness and elastic moduli of single-walled carbon nanotubes from frequencies of axial, torsional and in extensional modes of vibration, *Computational Materials Science* **47**: 1049-1059.

[6] Fatahi-Vajari A., Imam A., 2016, Torsional vibration of single-walled carbon nanotubes using doublet mechanics, *ZAMP* **67**: 81.

[7] Ferrari M., Granik V. T., Imam A., Nadeau J., 1997, *Advances in Doublet Mechanics*, Springer, Berlin.

[8] Fatahi-Vajari A., Imam A., 2016, Analysis of radial breathing mode of vibration of single-walled carbon nanotubes via doublet mechanics, *ZAMM* **96**(9): 1020-1032.

[9] Eringen A. C., 1972, Nonlocal polar elastic, *International Journal of Engineering Science* **10**: l-16.

[10] Basirjafari S., Esmaielzadeh Khadem S., Malekfar R., 2013, Validation of shell theory for modeling the radial breathing mode of a single-walled carbon nanotube, *IJE Transactions A* **26**(4): 447-454.

[11] Fatahi-Vajari A., Imam A., 2016, Axial vibration of single-walled carbon nanotubes using doublet mechanics, *Indian Journal of Physics* **90**(4): 447-455.

[12] Fatahi-Vajari A., Imam A., 2016, Lateral vibration of single-layered graphine sheets using doublet mechanics, *Journal of Solid Mechanics* **8**(4): 875-894.

[13] Ghorbanpour Arani A., 2015, Surface effect on vibration of Y-SWCNTs embedded on Pasternak foundation conveying viscose fluid, *Journal of Nanostructures* **5**(1): 33-40.

[14] Ghorbanpour Arani A.H., Rastgoo A., Ghorbanpour Arani A., Zarei M. Sh., 2016, Nonlocal vibration of Y-SWCNT conveying fluid considering a general nonlocal elastic medium, *Journal of Solid Mechanics* **8**(2): 232-246.

[15] Ansari R., Gholami R., Rouhi H., 2012, Vibration analysis of single-walled carbon nanotubes using different gradient elasticity theories, *Composites: Part B* **43**: 2985-2989.

[16] Ghorbanpour Arani A., Kolahchi R., Jamali M., Mosayyebi M., Alinaghian I., 2017, Dynamic instability of visco-SWCNTs conveying pulsating fluid based on sinusoidal surface couple stress theory, *Journal of Solid Mechanics* **9**(2): 225-238.

[17] Clerck J. D., 2014, *Topics in Modal Analysis I* , Springer, Cham.

[18] Gopalakrishnan S., Narendar S., 2013, *Wave Propagation in Nanostructures, Nonlocal Continuum Mechanics Formulations,* Springer, Cham.

[19] Huang J., Han Q., 2016, Controllable nanoscale rotating actuator system based on carbon nanotube and graphene, *Nanotechnology* **27**: 1-9.

[20] Mirtalaie S. H., Hajabasi M. A., 2017, Nonlinear axial-lateral-torsional free vibrations analysis of Rayleigh rotating shaft, *Archive of Applied Mechanics* **87**: 1465-1494.

[21] Cai K., Li Y., Qin Q.H., Yin H., 2014, Gradient less temperature-driven rotating motor from a double-walled carbon nanotube, *Nanotechnology* **25**: 1-6.

[22] Ebrahimi F., Shaghaghi Gh. R., 2015, Vibration analysis of an initially pre-stressed rotating carbon nanotube employing differential transform method, *International Journal Advanced Design and Manufacturing Technology* **8**(4): 13-21.

[23] Ishida Y., Yamamoto T., 2012, *Linear and Nonlinear Rotordynamics*, Wiley-VCH, Weinheim.

[24] Nahvi H., Boroojeni M.E., 2013, Free Vibrations of a rotating single-walled carbon nanotube embedded in an elastic medium based on nonlocal elasticity theory, *Acta Physica Polonica A* **123**: 304-306.

[25] Hayat T., Haider F., Muhammad T., Alsaedi A., 2017, Three-dimensional rotating flow of carbon nanotubes with Darcy, *Forchheimer Porous Medium* **12**(7):e0179576.1-e0179576.18.

[26] Pradhan S.C., Murmu T., 2010, Application of nonlocal elasticity and DQM in the flapwise bending vibration of a rotating nanocantilever, *Physica E: Low-dimensional Systems and Nanostructures* **42**(7): 1944-1949.

[27] Murmu T., Adhikari S., 2012, Scale-dependent vibration analysis of prestressed carbon nanotubes undergoing rotation, *Journal of Applied Physics* **108**(12): 123507.1-123507.7.

[28] Narendar S., Gopalakrishnan S., 2011, Nonlocal wave propagation in rotating nanotube, *Results in Physics* **1**(1): 17-25.